Reviewer #1

RC1.1: “The manuscript deals with radon progeny measurements in the High Arctic. The subject is certainly interesting to the readers of ACP and the data obtained during the field work is rare. My main comment is related to the instrument calibration. The results are presented as count rate per cubic meter. The authors should try to convert these to activity concentration units, otherwise comparing the data to other radon progeny observations is impossible. I understand the difficulties associated with this, detector efficiency for different nuclides, variations in the radon progeny disequilibrium etc. Still, the authors should do this, even with bold assumptions. One way would be comparing the operated instrument to other type but calibrated instruments. This would allow the comparison of activity concentration results to other observations in the Arctic area.”

We know that activity conversion is a bold limitation, but we are interested on variations not only on absolute determinations. We cannot move easily radioactive materials, useful for the calibration procedure, to Svalbard island and we are not in contact with groups with different instruments that can support interesting intercomparison with our setup. We know that conversion is important and for this reason we expressed activities in mBq m-3 even with the bold assumptions expressed in a note (*).

RC1.2: “Hasn’t there been a Heidelberg radon monitor at Mt. Zeppelin monitoring station at Ny-Ålesund?”

We found some projects (ARCTOC and RIS-1035) declaring the activity you are mentioning but no data and publications are easily accessible. We found the project report where radon is included but any result is described.

RC1.3: “I believe the terms NORM and TENORM are usually used with materials associated with human activities, not radionuclides in the atmosphere. An example is oil drilling sludge containing lead-210 or radium-226.”

We removed NORMs form the text and referred only to “naturally-occurring radionuclides”.

RC1.4: “The terms Sβ, Lβ, and Cβ could be replaced with appropriate IUPAC names after the calibration procedure mentioned above.”

The used terms were defined considering half-life of possible radionuclides. We expressed Sβ and Lβ in terms of $^{214}Pb_{eq}$ and $^{212}Pb_{eq}$ adding an “eq” suffix in order to distinguish our results stating the bold assumption of equilibrium between nuclides.

RC1.5: “In the literature reference list Sthol should be corrected to Stohl.”

Done

Reviewer #2

RC2.1: “Define Sbeta, Lbeta and Cbeta at the first appearance. Actually they are defined much later, above Eq. 5.”

Done in page 2

RC2.2: “Do not use “radon daughter”. Instead should be used “Radon progeny”.”

We fixed this indication

RC2.3: “Please give more details about Eqs. 6. How were these equations derived. From methodology section is not clear whether particular radon/thoron progeny determined, (i.e. could you determine Po218, Pb214 BI214 etc) or you determine just total sum of beta counts due to radon, thoron and cosmogenic nuclide.”

Equations from 1 to 7 are theoretical formulations that explain how to obtain the operational equations 8a,b,c. We have gross beta counts and we try to separate three different contributions depending on the specific half-life of nuclides. We cannot determine directly the separated activites of each isotope.

RC2.4: “Above Eq 1 was written that Tbeta is number of beta particles emitted by different nuclides. However, later in Eq 7, Tbeta has somewhat different meaning. In Eq. 7 Tbeta˛ is number of counts due beta emitters in first and fourth measuring intervals.”

We checked definitions in order to be coherent. Tbeta in Eq.1 is the sum of beta particles generated by different nuclides (see text in P3 L3). It is the sum of three defined radioactive components Sbeta, Lbeta and Cbeta above Eq.5 and if we consider different counting intervals (the first and the forth) we have to specify Tbeta as mentioned in the text for Eq 7.

RC2.5: “In Eq. 7 progeny concentration was multiplied with detection efficiency which produce count numbers. What is the sense of decay parameters (ðİŚŚðİŚŰðİŚŻ) in Eq. 7 is not clear, please explain. I have experience with radon progeny measurements from beta emitters on filter. Very often, some physically non realistic results were obtained- due to i) variation of detection efficiency because of beta spectrum changing during the counting, and ii) counting statistic which is important source of errors particularly when the count rate is small. Authors devote significant care to the variation of detection efficiency, but the second fact is unavoidable. I can assume that count rates in measuring intervals are small, due to small radon concentration in open space. Then, statistical variations are large while this method is very sensitive on the number of counts. I would like to know did authors meet some physically unacceptable results or not.”

The decay parameter is a coefficient derived for each counting interval considering the sampling phase (Eq.2) and counting phase (Eq.4). We specified this relation in the text. The counting statistics is of course important when activities are low and this issue represents a limitation of this technique especially regarding the long-lived progeny and the near-constant progeny. The background levels of those components are probably close to the specific LLDs and an high-frequency bias can occur due to this limitation.

RC2.5: “Bellow Eq. 9 was written “The estimation of the three components was obtained minimizing the chi squared indicator, calculated between the four counting intervals and the respective values simulated between the two endmember situations“. Can you explain in more details what is the meaning of the previous sentence. From this sentence follows that values were simulated. Then what was the purposes of the measurements. Counts obtained in 2nd and 3rd intervals were not used in calculations. Does this mean that those counts were taken from simulation (not from measurements) in order to avoid physically non realistic results."

We clarified in the text that while the endmembers situation were defined considering only the 1st and 4th counting intervals, the final estimation of the three components were selected considering the RMSE calculated using all of the four observed counting intervals. This procedure supported the minimization of biases associated with low counting levels. When counting levels were low we still have an high frequency bias that can be removed only having a solid calibration procedure and possibly an intercomparison with an independent technique.

Reviewer #3

RC3.1: "For example, perhaps diurnal composite plots of the 3 activity concentrations could be prepared for the low and high emission periods, to see what (if any) regular structure is evident, and whether or not this structure can be explained by local diurnal changes in meteorology (which would also require diurnal composite plots of the meteorological components). Perhaps diurnal sampling windows are necessary to help distinguish between local and remote phenomena under some conditions?"

We considered short-lived activities above the 90th percentile, the most stable atmospheric conditions, and any diurnal pattern is evident during the two emanation periods, coherently with the length of the daylight (about 24 hours) during the considered period. Except for air temperature, meteorological parameters (absolute humidity and wind speed) and activities are almost stationary in the composite plot. There are of course high-frequency turbulences but making averages, this information is lost. More detailed information must be acquired in order to investigate diurnal patterns but the complexity of the fiord system dominates on the diurnal variations.

RC3.2: "Speaking of local processes, there is significant topography (order 1000m) adjacent the observation site. Do calculated absolute humidity values and diurnal wind speed/direction indicate the occurrence of katabatic drainage flows at any times of the observation period?"

Topography of Svalbard, focusing the attention specifically to the study site, is characterized by the maximum elevation of about 1000 m a.s.l. and the presence of small glaciers (below 100km2) close to the observatory. The meteorological description of the site [Beine et al 2001; Argentini et al 2001] associates the dominant source of katabatic events with the Kongsvegen (105km2) / Kronebreen (690 km2) glaciers, located to the eastern sector of our site, 15 km far from our facility. There is of course a WNW wind component related to the open sea and secondary slope stream from the SW direction associated with the Broeggerbreen (6 km2) and the Blomstrandbreen (18 km2) glaciers. The katabatic events are more frequently during the winter season and they are almost absent during the summer. A strong channelled behaviour of the wind pattern can be observed due to the morphology of the studied fiord but the penetration of katabatic winds below the inversion layer (ranging between 200 and 500 m a.s.l.) is not so frequent. Esau and Repina (2012) observed a decoupling of wind patterns at the ground and above the inversion layer and associate this behaviour also to the presence of sea ice in the fiord. We added to figure 4 also the panel showing the wind direction and the absolute humidity and commented the observations in section 3.1.

RC3.3: "If these flows are bringing to the surface air of recent tropospheric origin under certain conditions, is this contributing to the Cβ observations in any way? The authors allude to orographic effects at the site on P8 L8-9, but make no effort here to investigate the possibility further."

We analysed the relation between radioactive components and meteorological parameters and high-Cβ events started when significant absolute humidity reductions and wind speed increments occurred. Furthermore, the study site represents a complex system as described in the text and the dominant direction of origin concerning high-Cβ transport is ESE.

RC3.4: "Since the Cβ activities appear so disconnected from the behaviour of the radon progeny, it would be interesting if the authors could say something about what the main driving factors for the observed Cβ activity actually are at this site."

We observed events that can be related to glacier streams (see R3.3) and we can also suppose a contribution of the inversion layer to the income of Cβ-enriched air masses but further information must be gathered in order to fully analyse this contribution to the fiord system.

RC3.5: “The authors need to invest more effort to effectively separate local and remote terrestrial influence on their observations (more detailed than the present Fig 3 summary). For example, an hourly ratio between thoron and radon would provide a relative measure of local vs remote influence. Such data could be plotted against wind speed to see whether a wind speed threshold could be used at this site to better separate local and remote influences (after deciding upon a L:S ratio threshold to separate local from remote influences).”

Two separate thresholds can be defined for each emanation period. This indication is connected also to the wind direction and for this reason we substituted Fig.3 with bivariate polar plots containing the S:L ratio.

RC3.6: “Local and remote influences could be separately investigated in more detail. For example, a better relationship between simulated local source strengths and observed activities might be obtained if a wind speed threshold was used to isolate the local signal. Likewise, a more comprehensive (and statistically robust) trajectory analysis (than the present “analysis” that appears to be based on 4 individual trajectories), could be performed on remote terrestrial influences if high Sβ activity periods were targeted within periods of identified remote influence (based on the determined wind speed threshold or L:S ratios).”

The definition of a wind threshold is controlled also by the wind direction (new Fig.3) since wind coming from the open sea (NW) are less influenced by local contributions compared with air masses coming from the glacier (ESE) that can flow over land much more than oceanic masses. This last origin can involve or not the inversion layer and additional information, absolute humidity do not completely describe this dynamics, are required.

RC3.7: “Plotting the previously mentioned ratios (S:L, S:C, L:C) along with wind speed and direction might also help with a more detailed interpretation of the information summarised in the current Figure 3. Certainly, the “age” of the radon in the sampled air could be effectively demonstrated using the hourly L:S ratio, and periods when the thoron contribution is low (due to a distant influence) could be targeted for separate investigation.”

We described the new Fig.3 in the text.

RC3.8: “To assist with the authors’ intention of further investigating the effects of atmospheric stability on observed activity variability at this site resulting from local contributions, they might consider selecting a defined portion of data (say the period of high radon activity within the first 2 weeks of August), and re-plotting just this portion (so that data features are clearer) along with the corresponding wind speed, temperature and absolute humidity. If there are extended times within this two week period when wind speeds are ≤3 m s-1, then the authors might consider approximating and removing fetch effects as described in Chambers et al. (2015), and investigating the resultant diurnal variability of radon activity for radon accumulation periods. They may have some success in relating these radon accumulation periods to their predicted fluxes (if estimates of mixing depth can be made).”

The suggestion is interesting but an adaptation of Chambers et al (2015) is required since diurnal patterns are very limited. We would focus the attention on accumulation periods (the duration can cover up to 20 days during summer) in the next future.

RC3.9: “P1 L10-11: The authors draw attention to the stringent requirements of radon lower limit of detection for measurements in the Arctic. Briefly in the Introduction, for context, the authors might like to quantify what they believe to be the required LLD for observations of this kind in the Arctic, how this differs from LLD requirements in the Antarctic, and why this is the case (making reference to the potential range / restrictions of possible terrestrial-free fetch; since this is pertinent to their general interest in pollution transport to Arctic regions).

We added to P1 the text in L5-10.
added ref Samuelson et al 1986

RC3.10: “Radon concentration thresholds for “baseline” (minimally terrestrially influenced) or “regional background” air masses are becoming more clearly established (see, for example, Chambers et al. 2016a and references therein). Since calibrated activity concentrations are not provided in this study it makes it harder for the reader to estimate, relative to other studies, the degree of recent (within the past 2 weeks) terrestrial influence from unfrozen surfaces the observed air masses have experienced. Can the authors help to bridge this gap by approximating what range of radon concentrations their observed radon activity values in Fig 2 represent?”

We updated Fig.2

RC3.11: “P1 L12: A claim to uniqueness of this study is the ability to resolve, at hourly temporal resolution, the activities of different radon progeny (220Rn, 222Rn) at concentrations typical of the Arctic. But aren’t there other readily available single-filter radon progeny detectors that capable of doing the same? One example that comes to mind is the Heidelberg Radon Monitor (HRM; Levin et al. 2002); the output of which can be readily calibrated to radon progeny activity concentrations. HRM’s have been successfully deployed and operated at several Antarctic bases (for which LLD requirements are more stringent than in the Arctic). If the FAI Instruments PBL mixing monitor (in the configuration adopted for this study), has capabilities significantly beyond those of other such monitors, it would indeed be worthwhile for the authors to make this point clearly. Furthermore, direct electrostatic deposition monitors (e.g. Wada et al. 2010; Grossi et al. 2012) are also capable of separately resolving these radon isotopes, are relatively portable, require no assumptions about the degree of equilibrium between radon and its progeny, and have a lower limit of detection comparable to the FAI PBL mixing monitor. Does the PBL mixing monitor have any particular advantages over these kinds of detectors? (I ask this question in relation to the quote from the authors that I have copied below in my comment on “P2 L30-32”)

We specified in the text that our measurements are the first in the Arctic region, defined by latitudes above 70°N. We found the ARCTOC projects and the relative activity in the RiS portal (RIS-1035) declaring attempts to measure radon in Svalbard but no data are easily accessible (no results are present also in the project report). The northernmost dataset is located in Pallas (Finalnd) but latitude is 68°N (Schmithüsen et al. 2017) and the location is a continental site. Levin et al 2002 made observations below 60°N.

RC3.12: “P1 L 28-29: Some other articles pertaining to the application of radon observations in atmospheric stability analyses that may be of interest to the authors include Williams et al. (2016), Wang et al (2016), and Chambers et al. (2016b,c).”

We added refs of interest.

RC3.13: “P2 L 4: Regarding detectors capable of very low level radon detection for polar or high-altitude environments, and their applications, the authors can find further, more up to date, information in Williams & Chambers (2016); Chambers et al. (2016a).”

we added refs

RC3.14: “P2 L6: Regarding direct detection methods. The direct ANSTO dual-flow-loop two-filter radon detectors actually observe the alpha decay of both the 218Po (t0.5 ∼3 min) and 214Po (t0.5 ∼20 min) progeny of 222Rn (see Griffiths et al. 2016 for details). However, since they are incapable of distinguishing between alpha particles of different energy, thoron (220Rn) is removed from the sample air prior to entering the detector. Detector response time issues related to the half-lives of the two radon progeny mentioned above can be completely corrected for as described in Griffiths et al. (2016). Importantly, direct techniques generally observe radon progeny formed under controlled (aerosol-free) conditions within their measurement delay volumes where radon gas is in equilibrium with its unattached progeny.”

We added ^{214}Po to the text and we specified the direct methods foresees a delay volume for obtaining controlled aerosol-free conditions during the measurement.

RC3.15: “P2 L9: Since radon is a noble gas, presumably it is the physical rather than chemical behaviour of radon upon which these techniques rely?”

We changed “chemical” to “physico-chemical” behavior of radon and specified later the radon is “physically-fixed” on aerosols.

RC3.16: “P2 L12: The way the parentheses are placed here makes it seem like radon and thoron are their own decay products.”

We anticipated the description of radon decay-half lives to P1 L26 in order to avoid misunderstandings.

RC3.17: “P2 L19: Reference missing for the citation of Wada et al. (2010). Please check all references.”

We added this ref

RC3.18: “P2 L19: As described in Williams and Chambers (2016) the lowest detection limit for continuous, high temporal resolution, environmental atmospheric radon concentration measurements is actually less than 10 mBq m-3; not 70 mBq m-3 as quoted by the authors. However, the 5000 L detector capable of such observations is strictly one of a kind, and operates only at the Cape Grim Baseline Air Pollution Station. The lowest detection limit for a routinely available ANSTO dual-flow-loop two-filter radon detector (the 1500 L model) is around 25 mBq m-3 (see, for example, Chambers et al. 2014; 2016a). When response time corrected (as per Griffiths et al. 2016) these detectors have a temporal resolution of 30 minutes and an absolute accuracy of around 10% at radon concentrations of 100 Bq m-3 (as described in Chambers et al. (2014) this accuracy further improves for longer averaging times or higher concentrations).”

We updated the LLD with the one declared in Williams and Chambers (2016) referencing to Griffith et al (2016) that is more easily accesssible.

RC3.19: “P2 L22: Please note that the terms Sβ, Lβ and Cβ have not yet been defined in the manuscript.”

We substituted the not-declared terms with short-lived, long-lived and near-constant progenies.

RC3.20: “P2 L23: I feel that this brief review of radon detection technology is incomplete without mention of the Heidelberg Radon Monitor (Levin et al. 2002; see also Schmithüsen et al. (2017) for a discussion of many of the research-grade radon detectors currently operating throughout Europe;

details of the ARMON electrostatic deposition detectors operating in Spain are available in Grossi et al. 2012)."

We added Levin et al (2002) and also Paatero et al (1994) to the review

RC3.21: "P2 L25: ". . . the lowest detection limits can [only] be obtained having a complex sampling/counting system that is difficult to deploy and maintain in remote conditions" I believe that this statement is incorrect. The only disadvantages of two-filter detectors (capable of the lowest detection limits) are (i) that they are not readily portable (after having been installed), on account of their large size (2-3m), and (ii) and that they measure only Radon-222 (since Radon-220 is removed from the sampled air stream prior to entering the detector). 220Rn removal is necessary because their alpha counting system can't distinguish between ï A ¸ a-particles of different energy. The operation of the two-filter detectors is not complex; it is based primarily on a ZnS-photomultiplier counting system, a pair of centrifugal blowers, and a Campbell data logger. As such, power requirements are limited to around 100-120W at 240V when sampling from close to the surface. In spite of their size, these detectors weigh only around 100 kg, and can be readily deployed in challenging remote sites (from mountain-top to polar regions) or mobile platforms (such as ships). Furthermore, where network services are available they can be fully remotely controlled. Since calibration and instrumental background checks on the two-filter detectors are performed automatically (or via remote control), maintenance requirements are also minimal. In fact, a 1500 L model two-filter radon detector has been in service in Antarctica since February 2013 to current (October 2017), and the only user intervention required over this >4-year period has been to remove ice collected on the inlet tube on two occasions. Over this time the detector's calibration has remained quite stable, as has the lower limit of detection (25-30 mBq m-3). In most situations, however, we have found it prudent to replace the sensitive components of the two-filter detector's measurement head every 5 years to maintain a high sensitivity and low instrumental background."

We clarified advantages and disadvantages in the text P3 L2-5.

RC3.22: "P2 L28-29: Particular assumptions regarding the degree of equilibrium between radon and its progeny will also change under high humidity (or indeed foggy or hazy) conditions, and (during the summer months at this site when local emissions are significant), depending on the height above ground at which sampling is conducted."

We modified the text considering that high-humidity conditions include precipitation events.

RC3.23: "P2 L30-32: "This is a single-filter approach coupled to beta-counting and it represents, at the moment, the best compromise between detection efficiency and required resources." This claim, I feel, is somewhat misleading. As previously mentioned, two-filter detectors have low power requirements, minimal maintenance requirements, a 30 minute temporal resolution, require no assumptions to be made about the state of equilibrium between radon and its progeny, an average measurement sensitivity that rarely changes by more than 1% per year (in a roughly linear, correctable manner), and have a detection limit almost an order of magnitude better than that of the FAI PBL mixing monitor. They are, however, large (if space is an issue at the measurement location), not designed to be portable (which is only really a concern for short-term campaigns, since unpacking and initial setup can take 2 days), and they are not capable of monitoring activity concentrations of thoron progeny, or cosmogenic radionuclides. In summary, there are some advantages to using the PBL mixing monitor rather than a two-filter detector in some situations, but I think these relate more to its portability and ability to distinguish between different progeny than to resource requirements (e.g. maintenance and power)."

We clarified earlier the advantage of distinguish the different progenies and we specify at this point that the best compromise is referred to our logistics

RC3.24: “Interestingly, in their comparison of advantages/disadvantages between direct and indirect measurements, the authors fail to mention the apparent difficulty in obtaining consistent absolute radon activity concentrations from the instrument used in this study. Following claims that the instrument is readily deployable in remote environments, and that it requires minimal maintenance/resources, later (on page 5) the authors go on to say “Considering the logistic restrictions of the study site, routine quality check and sampling efficiency assessments were not possible.” Problems, apparently specific to this campaign, that have prevented the authors from reporting of absolute radon concentrations in this study. However, despite the established history in the literature of applying the FAI PBL mixing monitor for atmospheric radon sampling (and other similar single-filter β-radiation detectors of this kind, such as the OPSIS SM200 stability monitor), few of the published studies report calibrated (absolute) radon activity concentrations. It would certainly improve the utility of these devices for applications like the one described in this study if absolute calibration of the observations was routinely possible.”

We are planning to define routinely calibration of this kind of instrument and we are studying how to solve logistics and hardware problems. The main challenge is represented by the impossibility to have permanent personnel at the station during the whole campaign length.

RC3.25: “P3 L7: Regarding Figure 1b, this figure would be more useful to the reader if the view were “zoomed out” a little more. If the figure was changed such that the width represented 150-200 km, instead of about 50 km, then it would put the site in better context regarding the trajectory analysis and local influences, and would not lose too much of the local topographic detail.”

We added a new Figure 1. The study site is on the left since the open sea is in front of the site and no information are present.

RC3.26: “Section 2.1: since this study is not the first application of the FAI PBL monitor, please include only the detail and theory in this section that (i) has not already been published, and (ii) pertains to the unique features of the detector operation for this study (which, as I understand, is the increased temporal resolution of sampling). Perhaps all of the detail in this section is required (the authors would be the best judge), but if other publications summarise the theory of operation (as much as it is similar to the FAI PBL mixing monitors with the slower temporal response), then it would be sufficient to refer the reader to other published works for an overview of the theory or principle of operation. This may leave more room for a more detailed analysis of the observations later.”

The algorithm presented here is all original. The theory is necessary for the reader in order to appreciate the introduction of the third radioactive component while the FAI PBL provides a 2-component output. The FAI algorithm is efficient at lower latitudes where the near-constant progeny is negligible.

RC3.27: “P6 L10-12: Can the authors provide any indication of how “good” the remote soil moisture estimates are? Was there any ground-truthing performed (either for this study or in the literature)? A reference to a study where the technique has been evaluated would be sufficient if nothing specific was tested in this study.

We added suggest Brocca et al. (2017) as reference.

RC3.28: “P6 L16: Could the authors comment briefly on the results of the comparisons of trajectory calculations between 500 and 1000m that led them to their final choice?”

We modified Fig.4 and commented the picture in text using the residence time of air masses at different altitudes. The interest on 1000m altitude is caused by the impact of the inversion layer on the mixing between lower and upper air circulation in the fiord system. Furthermore, there are no large differences between residence time over Svalbard estimated for 500 and 1000 m altitudes.

RC3.29: “P6 L22-23: “The evolution of the three radioactive components (Fig. 2a) seemed to be produced by the overlapping of different sources and processes.” This may well be the case, but little evidence to support this statement is provided in Figure 2a. Modelled local radon flux and air temperature are provided as companion series to the activity measurements, but there appears to be little in the way of direct consistent correlations between either of these two parameters and the more significant of the reported concentration variations in the measured activities. Perhaps including time series of wind speed, wind direction, ratios (e.g. between S:L, S:C, L:C), or trajectory-modelled time-over-land for each sample over the past 5 days would provide more information about factors contributing to the observed variability? Regarding Figure 2, please rethink the scale of the x-axis, consider decimal days or something similar. There appears to be little relationship between the axis tick marks and labels. This makes it hard to relate them to the data.”

We updated Fig. 2 and we included the requested information in Fig. 3 and Fig.4

RC3.30: “P6 L24-28: Various analyses are mentioned here, but there is no evidence of them in the figures (i.e. before/after plots showing the effect of what has been achieved, and why it was necessary).”

The seasonal separation (high and low emanation periods is highlighted by grey vertical lines. The first stated analysis consisted in separately treating the two periods. We modified Fig.2 plotting black dots for the raw data and we overlapped a trend with coloured lines.

<u>List of major changes</u>

- We revised the whole paper in order to improve the English writing.
- We prepared new Figure 1
- We prepared new Figure 2
- We prepared new Figure 3
- We prepared new Figure 4
- We modified the text of section 1 in order to fix point outlined by all the reviewers
- We clarified the rationale of equations 5 to 9 fixing numbering and some sentences
- We tried to support the conversion of activities in order to compare our results to literature, even if equilibrium and detector efficiency are still critical issues. We used bold assumptions and we evidenced this aspect using * for activities and the suffix “eq” for nuclides.
- We expressed, in section 3, activities in terms of mBq* in order to obtain absolute values
- We updated section 3.2 with the new figures and commented them in the text
- We updated and corrected the reference list.

High-time resolved radon-progeny measurements in the Arctic region (Svalbard Islands, Norway): results and potentialities

Roberto Salzano[1], Antonello Pasini[2], Antonietta Ianniello[2], Mauro Mazzola[3], Rita Traversi[4], Roberto Udisti[4]

[1]Institute for Atmospheric Pollution Research, National Research Council of Italy, Sesto Fiorentino (FI), Italy
[2]Institute for Atmospheric Pollution Research, National Research Council of Italy, Monterotondo (RM), Italy
[3]Institute of Atmospheric Sciences and Climate, National Research Council of Italy, Bologna (BO), Italy
[4]Department of Chemistry "Ugo Schiff", University of Florence, Sesto Fiorentino (FI), Italy

Correspondence to: Roberto Salzano (roberto.salzano@cnr.it)

Abstract. The estimation of radon progeny in the Arctic region represents a scientific challenge due to the required low limit of detection in consideration of the limited radon emanation associated with permafrost dynamics. This preliminary study highlighted, for the first time above 70°N, the possibility to monitor radon progeny in the Arctic region with a higher time resolution. The composition of the radon progeny offered the opportunity to identify air masses dominated by long-range transport, in presence or not of near-constant radon progeny instead of long and short lived progenies. Furthermore, the different ratio between radon and thoron progenies evidenced the contributions of local emissions and atmospheric stability. Two different emanation periods were defined in accordance to the permafrost dynamics at the ground and several accumulation windows were recognized coherently to the meteo-climatic conditions occurring at the study site.

1 Introduction

The detection ~~Monitoring the levels~~ of radionuclides within the Arctic environment is an important tool to help understanding the pathways for radionuclide transport to, within and from the Arctic (Chun, 2014; AMAP, 2010). Naturally~~-~~ o~~O~~ccurring radionuclide~~Natural Occurring Radioactive Materials (NORMs)~~s, emitted by ~~are nuclides strictly related to~~ geologic sources and associated with cosmogenic processes, ~~which~~ can describe air-masses origin and residence time (Baskaran, 2016). This is a key information for studying the fate of pollutants in the Arctic region, which is controlled by the meteo-climatic conditions occurring in the different seasons and in the different days of the year (Baskaran and Shaw, 2001). From a seasonal point of view, the extension of the so-called *"Arctic front"* (Stohl, 2006) can deflect, in fact, air masses originated in continental areas (such as Northern Europe, Russia, Asia and North America) to higher altitudes, reducing the contribute to the deposition processes. Radon (^{222}Rn and ^{220}Rn have half-lives, respectively, of about 3.8 days and 55 s)~~Radon~~ and its progeny represent an important tracer of the meteo-climatic conditions occurring in the lower atmosphere. The use of naturally-occurring nuclides~~NORMs~~, and in particular of radon, for pollution purposes was extensively investigated at lower latitudes (Duenas et al., 1996; Perrino et al., 2001; Sesana et al., 2003; Chambers et al., 2011; 2015), especially in urban settings. These case studies support the scientific community to use ^{222}Rn as a comparatively simple and economical approach for defining the stability conditions of the lower troposphere and for estimating the mixing height (Pasini and Ameli, 2003; Sesana et al., 2003; Veleva et al., 2010; Griffith et al., 2013; Pasini et al., 2014; Salzano et al., 2016). The low emissive conditions of the ground, controlled by the permafrost dynamics, limit the application of this approach in ~~polar regions~~Polar Regions. The expected radon activities in the air (we refer to especially to 222Rn that is more frequently estimated in literature) ranges in the Arctic between -30 mBq m^{-3}, with persistent polar winds, and more than ~~up to~~ 400 mBq m^{-3} when continental air masses reached higher latitudes (Samuelson et al., 1986). This value is, of course, influenced by the latitude, by the meteo-climatic conditions, by the altitude of the sampling site and, finally, by the distance of continental areas. This range~~equirement~~ is coherent with Antarctica ~~(Chambers et al 2014)~~ when "oceanic" air masses occurs and it is less stringent when "continental" or "local" air messes are incoming (Chambers et al., 2014). The occurrence of a melting season coupled with the higher extension of bared local and remote soils, potential sources of radon emissions, let the requirement of~~.~~ ~~The requirement of~~ significant low levels of detection (LLD) less stringent in Svalbard islands. The approach to t~~T~~he reduction of LLD can, in fact, be based on~~bypassed only~~ having high-volume sampling and/or high-sensitivity detectors (Chambers et al., 2014). The available techniques can be classified considering the half-life ($t_{1/2}$) of the considered isotopes. A first methodology is based on ~~:—~~the direct meas~~s~~urement~~measurement~~ of radon nuclides (^{222}Rn or ^{220}Rn) detecting the in-equilibrium progeny (^{218}Po, ^{214}Po and ^{216}Po, with $t_{1/2} < 20\cancel{5}\ min$). Some ~~;); the~~ indirect techniques include~~based on~~ the detection of short-lived isotopes (such as ^{214}Bi and ^{214}Pb, with $t_{1/2} < 1\ hour$) and of long-lived nuclides (such as ^{212}Bi, ^{212}Pb with $1 < t_{1/2} < 10\ hours$). Finally, some ~~;); and the ind~~indirect~~indirect~~ methods are based on the detection of near-constant progeny (such as ^{210}Pb and ^{210}Bi, ~~with~~ with $t_{1/2} > 1\ day$). The main advantage of the direct measurement consists in the formation under controlled (aerosol-free) conditions where radon is in-equilibrium with its unattached progeny. Furthermore, the direct methods differ from the others by the introduction of delay volume necessary for the removal of not-in-equilibrium progeny. T~~All of these techniques are based on t~~he physico-chemical behavior of radon is the key feature in all of these techniques: it is a noble gas that, once emitted by soil, leaves the surface by molecular diffusion or by convection, and enters the atmosphere where ~~it is distributed by~~the turbulent mixing diffuses nuclides (Porstendorfer, 1994). This gas is chemically unreactive and physi-sorption through electrostatic attraction on particles is ~~a~~ negligible ~~amount can be adsorbed on particles by physi-sorption through electrostatic attraction~~ (Bocanegra and Hopke, 1988). On the other hand, the radon decay products ~~(^{222}Rn and ^{220}Rn have $t_{1/2}$, respectively, of about 3.8 days and 55 s)~~ are metallic elements that are easily ~~physically fixed~~physically fixed to existing aerosol particles in the atmosphere. ~~The reduction of these particles in the atmosphere occurs either~~Either the reduction of these particles in the atmosphere occurs by radioactive decay or by removal processes (dry deposition, rainout, washout). Furthermore, turbu~~r~~lent mixing controls t~~T~~he distribution of this aerosol component in the troposphere ~~is controlled mainly by turbulent mixing~~.

Different techniques allow ~~Different techniques were developed for the~~ estimationg~~estimation~~ of this important tracer, all of them based on ~~considering~~ the physical behavior and/or the decay chain of this gas. ~~The most common "*direct*" measurement of Rn is based on~~ T~~t~~he collection of ^{218}Po by electrodeposition coupled to alpha-particle detection (Wada et al., 2010) represents the most common “*direct*” measurement of Rn.~~).~~ Furthermore, the lowest detection limit (below~~up to~~ ~~70~~ 10 mBq m^{-3}) can be obtained isolating the gaseous phase, removing the ^{220}Rn component and detecting the freshly-decayed metals (Griffith et al.~~Chambers et al.~~, 2016~~12011~~). Looking at the “*indirect*” measurement of Rn on particulate matter, the most common approach is based on collecting and counting the total activity associated with the short-lived (S_β) ~~$S\beta$~~ and the long-lived (L_β) progenies~~L_β~~ (Paatero et al., 1994; Perrino et al., 2000; Levin et al., 2002; Salzano et al., 2016). The determination of the near-constant (C_β) progeny completes, in conclusion, t~~T~~his picture. ~~and t~~The ~~is completed, in conclusion, by the determination of the near-constant (C_β) progeny C_β, where the~~ collection and the detection steps, in this case, can be separated and samples can be stored for a significant time (Paatero et al., 2010). Considering advantages or disadvantages, the lowest detection limits can be obtained having a relatively more complex sampling/counting system that requires more space ~~is difficult to~~for the installation. ~~deploy and maintain in remote conditions~~ The availability of an accurate instrument implies the requirement of reliable calibration procedures that in remote areas could be restricted by logistic reasons, as in our case. Furthermore, the “*direct*” systems cannot detect ^{220}Rn decay product due to the impossibility to separate contributions using alpha detectors. ~~.~~ The “*indirect*” methods have, on the other hand, ~~-~~a reduced impact in terms of resources necessaries for the installation and for maintenance but they require the assumption of equilibrium between radon gas and its aerosol progeny. This assumption is generally considered suitable~~to be valid~~ for sites that are at a significant distance from the radon terrestrial source, when the sampling height from the ground is significant, if weather conditions are fairly calm, but is likely to fail under high-humidity and severe-sea conditions~~during precipitation episodes and under severe-sea conditions~~. This study will focus the attention on the technique based on the not-in-equilibrium progeny ~~(S_β, L_β and C_β)~~, where high-volume sampling is not required. This is a single-filter approach coupled with~~to~~ ~~beta-counting~~beta counting and it represents, ~~at the moment~~now, the best compromise for our logistic resources between detection efficiency and required man intervention~~resources~~. Furthermore, the disequilibrium issue is less invasive compared with the most common approach available in literature about the Arctic region (Zhang et al., 2015), where near-constant progeny is involved.

The present study tests the potentiality to study hourly variations instead of daily samples. Different authors ~~Seasonal trends~~ have ~~been~~ already investigated seasonal trends highlighting ~~and~~ the role of the Arctic haze on radon and its progeny ~~has been already highlighted~~ (Suzuki et al., 1996; Paatero et al., 2010; Zhang et al., 2015). We will describe the high-frequency behavior of radon progeny looking at the persistence of stability conditions and we will combine these results with the air-mass characterization based on back-trajectories.

2 Methods

The study was carried out at the Gruvebadet observatory, facility of the Arctic Station “Dirigibile Italia” located in Ny Ålesund, Spitzbergen (79°N, 11°E, 50 m a.s.l.). The site (Fig. 1) is located in the Brøgger Peninsula that is NW-SE oriented in front of the Kongsfjorden. Different glacial valleys (Austre - Midtre - Vestre Lovénbreen, Austre Brøggerbreen, etc.) slope down from the reliefs where the highest altitude is 1017 m above the sea level. Additional facilities are available nearby for the characterization of the physical conditions of the lower atmospheric boundary layer. The survey covered the period from 1 April to 28 October 2015, including the melting season and the entire summer season.

2.1 Radon progeny

The natural radioactivity was measured using an automatic stability monitor (PBL Mixing Monitor, FAI Instruments, Fontenuova, Rome, Italy) with a sampling height of 3 m above the ground. The system comprises an air sampler for the collection of particulate matter on filter membranes and a Geiger-Muller counter for determining the total β activity of radionuclides attached to the particles. The instrument operates on two filters at the same time: while the sampling phase is acting on one filter for 1 h, another filter is performing the β detection ~~is performed on the other filter~~ at four different intervals (0-10, 10-20, 30-40, 40-50 minutes). These instrumental features ensure that the β activity of the particles is continuously determined over an integration time of 1 h and that the β measurement period is long enough to guarantee highly accurate results. The automatic subtraction of the background radiation (Perrino et al., 2000) improves t~~T~~he accuracy of the determination ~~is improved by the automatic subtraction of the background radiation (Perrino et al., 2000)~~ and the maximum instrumental error at the lowest counting level was about 8%. T_β in Eq. (1) is the sum of β particles emitted by different nuclides sampled in the aerosol ($[N]_\beta^i$):

$$T_\beta = \sum_{i=1}^{n} [N]_\beta^i \tag{1}$$

Each nuclide is collected on the filter after a sampling period and it is detected during a counting interval. Differential equations (Islam and Haque, 1994) regulate b~~B~~oth phases ~~are regulated by differential equations (Islam and Haque, 1994)~~ and the sampling step~~phase~~ can be generalized as:

$$\frac{d[N]_s^i}{dt} = \nu[N]_{air}^i + \lambda_{i-1}[N]_s^{i-1} - \lambda_i[N]_s^i \tag{2}$$

~~where t~~The~~the~~ first term on the right side represents the collection obtained specifying the air sampling flow rate (ν) in m^3 h^{-1} and activity in the air ($[N]_{air}^i$). The second term defines the contribution of the ~~eventually-occurring~~eventually occurring parent isotope (i-1) on the filter and the third term is the decay component of the daughter nuclide (i). Those decay terms considers the specific decay constant of the parent (λ_{i-1}) and daughter (λ_i) isotopes. Furthermore, the presence of the nuclide in the air is described in Eq. (3) by the combination of the locally originated nuclide ($[N]_L^i$) added to transported contribute ($[N]_T^i$).

$$[N]_{air}^i = [N]_L^i + [N]_T^i \tag{3}$$

Similar differential equations describe t~~T~~he counting phases ~~are described by similar differential equations where~~and the daughter decay and the eventual supply of the parent nuclide control the β emission~~tting emitting is controlled by the daughter decay and the eventual supply of the parent nuclide~~:

$$\frac{d[N]_\beta^i}{dt} = \lambda_{i-1}[N]_s^{i-1} - \lambda_i[N]_s^i \tag{4}$$

Considering only naturally-occurring nuclides~~NORMs,~~, Eq.~~NORMs, Eq.~~ (1) can be described by the sum of β emissions produced by ^{222}Rn progeny (S_β), ^{220}Rn progeny (L_β) and some near-constant nuclides including cosmogenic isotopes (C_β).

$$T_\beta = [^{214}Pb]_\beta \cancel{S_\beta} + [^{214}Bi]_\beta \cancel{S_\beta} + [^{212}Pb]_\beta + [^{212}Bi]_\beta \cancel{L_\beta}\cancel{L_\beta} + C_\beta \qquad (5)$$

Excluding from C_β the contribution of ^{210}Pb, due to the low β energy emission ($E_\beta < 100\ keV$) where the detector has a very low efficiency (Lee and Burgess, 2014), the remaining near-constant nuclides are ^{210}Bi ($t_{1/2} \sim 5\ days$ and $E_\beta \sim 1162\ keV$), ^{10}Be ($t_{1/2} > 10^6\ years$ and $E_\beta \sim 556\ keV$) and ^{14}C ($t_{1/2} \sim 5700\ years$ and $E_\beta \sim 156\ keV$). While the ^{14}C contribution is limited by the low efficiency of detectors at low energies and by the limited amount of carbon present on filters (below 1 µg m^{-3}), the ^{10}Be component is limited by the low activities present in the atmosphere. Summarizing, we have one rapid-decay component (S_β decreases 60 - 70 % within one hour) and one near-constant member (C_β). The intermediate term (L_β) reduces its activity to about 5 - 15 % after one hour. The mixing between those three components defines the final decay behavior observable at an hourly scale with four different counting steps. We can have two different seasonal behaviors in the Arctic region. The first~~:~~ one~~: one~~ occurs ~~ring~~ ~~occurring~~ especially during the Arctic winter, when the local emission of radon (both ^{222}Rn and ^{220}Rn) is negligible ($L_\beta \simeq 0$) and the residence time of aerosol over sea (more than 2 days) is higher in presence of the so-called “Arctic haze” ($C_\beta > 0$ ~~$\simeq [^{210} \simeq [^{210}Bi]_\beta$~~). The second~~;~~ ~~);~~ one occurs~~sring~~~~occurring~~ especially in the summer, when the local component is significant and the Arctic haze is reduced ($S_\beta \gg L_\beta > C_\beta$). We assume under both conditions that transient equilibrium is occurring between the two progenies ($[^{214}Pb]_{air} = [^{214}Bi]_{air}$ and ~~-~~$[^{212}Pb]_{air} = [^{212}Bi]_{air}$). Some bias can occur especially during the summer when the local source is dominating over transport and the disequilibrium between progenies can be significant.

The Bateman's solutions support the development of the ~~above mentioned~~above ~~The above~~ mentioned differential equation Eq. (2)~~,~~ concerning the sampling phase~~, can be solved using the Bateman's solutions, considering the two seasonal assumptions~~:

$$[^{214}Bi]_S\cancel{]_\beta} = 1.51[^{214}Pb]_{S\cancel{\beta}} \qquad (6a)$$

$$[^{214}Pb]_{air} = 1.97\ \nu^{-1}\ [^{214}Pb]_S\cancel{]_\beta} \qquad (6b)$$

$$[^{212}Bi]_S\cancel{]_\beta} = 1.02[^{212}Pb]_S\cancel{]_\beta} \qquad (6c)$$

$$[^{212}Pb]_{air} = 1.03\ \nu^{-1}\ [^{212}Pb]_S\cancel{]_\beta} \qquad (6d)$$

$$C_\beta^{air}\cancel{[^{210}Bi]_{air}} = \cancel{\nu^{-1}[^{210}Bi}\nu^{-1}C_\beta\cancel{]_\beta} \qquad (6e)$$

The Eq. (4) regarding the counting intervals must be solved for each period. The solution must consider the first and the last counting periods: from 0 to 10 minutes (first interval T_β^1) and from 40 to 50 minutes (forth interval T_β^4) after the end of the air sampling.

$$T_\beta^1 = \epsilon_{1024}[^{214}Pb]_S\cancel{]_\beta}d_1^1 + \epsilon_{3272}[^{214}Bi]_S\cancel{]_\beta}d_2^1 + \epsilon_{570}[^{212}Pb]_S\cancel{]_\beta}d_3^1 + \epsilon_{2252}[^{212}Bi]_{\cancel{\beta}S}d_4^1 + C_\beta \qquad (7a)$$

$$T_\beta^4 = \epsilon_{1024}[^{214}Pb]_S\cancel{]_\beta} d_1^4 + \epsilon_{3272}[^{214}Bi]_S\cancel{]_\beta} d_2^4 + \epsilon_{570}[^{212}Pb]_S\cancel{]_\beta} d_3^4 + \epsilon_{2252}[^{212}Bi]_S\cancel{]_\beta} d_4^4 + C_\beta \quad (7b)$$

The coefficients in Eq. (7a and 7b) are the detector efficiencies at each energy (ϵ_{keV}) and the decay parameters (d_i^n) obtained solving exponential equations (Eq. 4) for each ith isotope at each nth counting interval. We were not able to determine routinely the detector efficiency at each energy but it was possible to make some experiments with a similar instrument and some reference materials such as a KCl standard (we prepared a known ^{40}K filter with $E_\beta \sim 1311\ keV$) and a ^{137}Cs-contaminated soil (we prepared a ^{137}Cs-enriched filter with $E_\beta \sim 531\ keV$ where the activity was determined by γ-spectrometry). This preliminary calibration requires a stronger effort for estimating precisely the efficiency at different energies but a relative ratio between the detector efficiency at 570, 1024 and 2252 keV normalized to the efficiency at 1024 keV was estimated in order to study the variations of the three β-emitting components (S_β, L_β and C_β). We found that $\epsilon_{570} \sim 0.41\epsilon_{1024}$, $\epsilon_{1162} \sim 1.1\epsilon_{1024}$, $\epsilon_{2252} \sim 1.8\epsilon_{1024}$ and $\epsilon_{3272} \sim 2.1\epsilon_{1024}$. Substituting these parameters to Eq. (7a and 7b) and solving the system including a ^{220}Rn to ^{222}Rn ratio (f), we obtained:

$$S_\beta = 1.97\frac{(N_{\beta,1} - N_{\beta,4})}{(2.15+0.74f)}\,\nu^{-1} \quad (8\cancel{9}a)$$

$$L_\beta = 3.74f\frac{(N_{\beta,1} - N_{\beta,4})}{(2.15+0.74f)}\,\nu^{-1} \quad (8\cancel{9}b)$$

$$C_\beta = [N_{\beta,4}\frac{(2.14f+1.89)}{(2.15+0.74f)}(N_{\beta,1} - N_{\beta,4})]\,\nu^{-1} \quad (8\cancel{9}c)$$

A~~where both all~~ll quantities are expressed in cps m^{-3}. Nevertheless, we prefer to enhance the contribution to the scientific community assuming the equilibrium between progenies during the observed period (~~and indicate~~ $^{214}Pb_{eq} = S_\beta$ $^{212}Pb_{eq} = L_\beta$ ~~v~~). Assuming also that ~~en~~$\epsilon_{1024} \sim 10\%$, having in mind that further efforts are~~is~~ necessary for a reliable calibration,~~s is necessary for a reliable calibration,~~the comparison of our results with literature is possible obtaining activities expressed in mBq m^{-3}. Regarding C~~This cannot be done for~~$_\beta$, the conversion requires ~~-~~a deeper knowledge about this component and we prefer consequently to keep relative counts.~~since it is necessary to~~ The minimiz~~estimation of the three components was obtained~~ation of~~where both quantities are expressed in cps m^{-3}. The estimation of the three components was obtained minimizing~~ the chi-squared indicator, calculated between the four counting intervals and the respective values simulated between the two end-member situations (~~ing t since it is necessary to a deeper knowledge about this component.~~ $C_\beta = 0$ or $L_\beta = 0$) stsupported the estimation of the three components.~~and 4th counting steps $C_\beta = 0$ and $L_\beta = 0$).~~ The optimization algorithm was developed in the R-Project programming environment (R Core Team, 2016)~~counting steps..).~~ The lower limit of detection, in terms of ^{222}Rn, of the stability monitor was estimated at 150 mBq~~0.0.15 Bq~~ m^{-3} (Salzano et al, 2016) using an independent technique.~~).~~ Considering the logistic restrictions of the study site, routine quality check and sampling efficiency assessments were not possible. These limitations forced us to express ~~the three components in terms of relative radioactivity (cps m^{-3})~~ $^{214}Pb_{eq}$ and $^{212}Pb_{eq}$ as mBq* m^{-3} ~~)~~and to estimate C_β as relative counts. The respective lowest limit of detections were 200~~indicated as~~ mBq* m^{-3}, ~~with a LLD of 0.0035,~~250 ~~0.013~~mBq* m^{-3} and 0.0~~072~~15 cps m^{-3}~~with alowest limit of detections were indicated as LLD of~~ ~~$^{-3}$~~, respectively.

2.2 Soil Rn-flux

The estimation of the soil Rn flux (ϕ) was obtained using a stationary model where the major controlling factors are the soil radon emanation power and the soil water saturation (Zhuo et al., 2008). The model, based on Equation 10, required as input parameters the soil temperature (T_S), the soil water content (S), the soil Ra content (R), the soil density (ρ_b) and the soil porosity (p). In addition to some constants that are included, such as the radon decay constant (λ) and the diffusion coefficient of radon in the air (D_0), the emanation power (ε) can be calculated following the equations described by Zhuo et al. (2008).

$$\phi = R\rho_b \varepsilon \left(\frac{T_S}{273}\right)^{0.75}\sqrt{\lambda D_0 p e^{-6Sp-6S^{14p}}} \qquad (9$$

~~(10~~)

Compared to the preliminary description presented in Salzano et al. (2016), the description of the soil thaw depth is a critical input parameter in cold regions. Permafrost can be idealized as a two-layer system where the upper active layer overlays a frozen water-saturated layer. From this perspective, we approached the problem considering the 9 m temperature profile provided by the Bayelva borehole (Paulik et al., 2014), which supported also the estimation of the average temperature of the active layer. Under-prediction can affect t~~T~~he developed model under unsteady conditions since it is a simplified solution ~~that could be influenced by under-prediction under unsteady conditions~~. Appropriate validating activities are required in order to evaluate the performance of this model. The estimation of the soil water content was approached using remotely sensed data provided by the EUMETSAT organization. We selected the soil moisture product obtained by the ASCAT sensor (Brocca et al., 2017), which is a real-aperture radar operating at 5.255 GHz (C-band) (EUMETSAT, 2015).

2.3 Back trajectories

The analysis of the back trajectories was approached calculating the air mass path with the HYSPLIT model (Stein et al., 2015). We considered 5 days~~'~~ trajectories using the GDAS meteorological dataset. Simulations were targeted on the study site at different altitudes (500 and 1000 m a.s.l.) in order to evaluate the circulation without the influence of orography on trajectories (Esau and Repina, 2012). This issue is extremely important considering the complexity of the studied fiord system and the extension of Svalbard island compared to the model resolution.

3 Results

Two different questions were approached in order to evaluate the potentialities in using radon-progeny in the Arctic region: what is the impact of permafrost dynamics on the radon detection in the air? How does the air mass trajectory control the signal detected in the lower atmosphere?

3.1 The contribution of the local soil flux to the air concentration

The evolution of the three radioactive components (Fig. 2 a, b and c) was the result of~~2a)~~ ~~seemed to be produced by~~ the overlapping of different sources and processes: local emission, oceanic income, slope flows and atmospheric stability.~~.~~ All of these factors can ~~have~~ehave different seasonal behaviors and this framework~~issue~~ highlighted the need of a time-series analysis. The first step consisted, in fact, in de-trending the time series isolating the local-source component, which is controlled by the emissive condition of the local surface. The remaining seasonal components (distinct in low and high emanation periods) where analyzed removing the high-frequency bias (hourly~~daily~~ oscillations) using a smoothing procedure based on a centered weighted moving average with a 24-hours window (Cowpertwait and Metcalfe, 2009). The main feature distinguishing the identified periods was the amplitude of variations concerning the natural radioactivity. While small fluctuations (up to 1 Bq*~~0.1 cps~~ m^{-3}) in $^{214}Pb_{eq\beta}$~~S_β~~ were detected during the low-emanation period, $^{212}Pb_{eq\beta}$~~L_β~~ seemed to be very close the LLD~~quite negligible~~ and C_β was frequently detected. The high-emanation period was characterized by sharp variations up to ~~0.~~8 Bq*~~cps~~ m^{-3} in terms of $^{214}Pb_{eq\beta}$~~S_β~~, by significant variations concerning $^{212}Pb_{eq\beta}$~~L_β~~ and by an occasionally detectable amount of C_β. The presence of ^{212}Pb~~L_β~~$_{\beta eq}$~~L_β~~ and C_β showed also a specific behavior: while the long-lived progeny$_\beta$~~L_β~~ followed the trend described by short-lived component~~S_β~~ (increasing from 26~~0.018~~0~~S_β (0.018 ± 0.013~~ mBq*~~cps~~ m^{-3} in the first period to 400~~and~~ mBq*~~and 0.06 ± 0.01 cps~~ m^{-3} in the second one), C_β showed the opposite (0.016~~09009 ± 0.007~~ cps m^{-3} in the first period and 0.015~~07007 ± 0.007~~ cps m^{-3} in the second one).

Furthermore, looking at peaks defined by values higher than the third quartile, different episodes can be identified for each progeny component during each emanation period. While the $^{214}Pb_{eq\beta}$~~S_β~~ and the ^{212}Pb~~L_β~~$_{\beta eq}$~~L_β~~ components showed episodes that are significantly matching in terms of maxima, especially during the high-emanation period ($r^2 = 0.79$), C_β showed peaks completely independent from the other components. The reconstruction of an indicative soil Rn-flux (Fig. 2d) supports ~~T~~the~~The~~ interpretation of the observed seasonality in the time-series~~ is supported by the reconstruction of an indicative soil Rn-flux (Fig. 2d~~~~b~~~~2b)~~. The two different emanation periods can be identified also looking at the soil Rn exhalation rate, which is controlled by the thermal behavior of the permafrost layer. The presented model output required two important input parameters (the thickness of the active layer and the average soil temperature) obtained from borehole measurements at the surface and from the ~~remotely-observed~~remotely observed water saturation of the ground. The final output of the stationary emanation model indicated a limited soil emission until the end of May with a maximal emissive condition of local soils reached after 30 days at the beginning of July. Referring to the impact of permafrost dynamics, we can distinguish between a low-emanation period (which includes the ablation, the fusion and active-layer development phases) and a high-emanation period (as soon as the ground reached the maximal thickness of the emanating active-layer). The transition between the two periods can be positioned approximately in 8-9 July 2015 within a very short time interval. The observed abrupt impact of soil emanation on natural radioactivity in the air is coherent with the expected stabilization of soil exhalation obtained from the model. This consistency implies that atmospheric processes are influenced by a regional source where emissive conditions of the ground are mostly stabilized. The model output is, in fact, representative only for the Ny Ålesund site as permafrost observations are ~~site-specific~~site-specific (the study area is a coastal zone),~~)~~ and they cannot describe the overall behavior of more internal areas where orography is very complex.

3.2 The contribution of the meteo-climatic conditions to the air concentration

The combination between the three components could represent a diagnostic tool capable to describe the meteo-climatic conditions occurred on air masses. Looking at the occurrence of isotopic mixtures with different relative percentage of each component~~ (Fig. 3a)~~, the most frequent situation during both emanation periods ~~(Fig. 3b) ~~was, of course, the condition dominated by the short-lived progeny~~ (HiS)~~, with a frequency ranged between 72% and 78%. The partition of contributions between the near-constant isotopes and the classes dominated by the long-lived progeny represented ~~T~~the~~The~~ most significant difference between the two periods~~ was represented by the partition of contributions between the near-constant (CS and SC) and the classes dominated by the long-lived progeny(HiL and SL) classes~~. While the intermediate conditions between short-lived progeny$_{\beta}$~~S_{β}~~ and C_{β} were more consistent during the low emanation period (respectively about 7% and 2%), the terms between short and long lived progenies$_{\beta}$~~S_{β} and L_{β}~~ were almost dominant during the second period (respectively about 15% and 26%). The first behavior is consistent with the end of the Arctic winter, when the ~~arctic ~~Arctic haze enriches polar air masses with nuclides such as ^{210}Pb and consequently ^{210}Bi (Zhang et al., 2015). Furthermore, those conditions could highlight the occurrence of “*old*” and/or high-altitude air masses that were persistent at higher latitudes where radon sources are negligible. On the other hand, the presence of the long-lived progeny $_{\beta}$~~L_{β}~~ could trace the contribution of local sources or the arrival of recently emitted air masses (this component has a limited residence time in the atmosphere due to its complete decay reached after 50 hours). The importance of detecting these different components consists in the possibility to estimate the “*age*” and the “*origin*” of air masses (Chun, 2014). The relationship between each radon-progeny mixture and the wind features highlighted (Fig. 3~~c~~)~~,~~ that~~when~~re the $^{214}Pb_{eq}$-$^{212}Pb_{eq}$ ratio wa~~i~~s~~ HiL situations were~~ strictly controlled by the occurrence of wind calm conditions. This diagnostic ratio increases, in fact, in correspondence of stagnant conditions when win speed was lower than 4 m s^{-1}. T~~Furthermore, t~~his pattern was particularly evident during the summer period (Fig.3b) when the ratio is higher than 10 under calm conditions and it was less pronounced during the melting season (Fig.3a) with values between 5 to~~and~~ 12. The arrival of oceanic air masses (NW) and ~~of ~~glacier-slope flows (NNE and ESE) contributed to reduce the ratio close to the LLDs ratio. Furthermore, it is important to notice that strong winds carried air masses with a lower content of radon progenies. This behavior was more significant during the melting season compared to the summer period and it implies~~ith3c) that HiL situations were strictly controlled by the occurrence of calm condition. Furthermore, this was particularly evident during the summer period with an occurrence of about 60%. On the other hand, this relation, observed also on the C_{β}-dominated mixtures, supports~~ that low wind-speed conditions favored~~favor~~ the accumulation of nuclides (atmospheric stability) compared to advective situations that moved all the components to the specific lower limits of detection. This observation is in contrast with C_{β}~~T~~, which can reach significant levels when advective conditions are associated only with glacier flows. Additional analyses were not possible at the moment since the near-constant component was very close to the estimated LLD and we can use this formation just as trigger of potential intrusion of higher tropospheric air masses. The study site is, in fact, deeply influenced~~ influenced deeply~~ by orographic effects and it can be described as a system that might be heavily stratified (Di Liberto et al., 2012; Esau and Repina, 2012; Mazzola et al., 2016). The role of wind-calm conditions was relevant if we consider that near-stable conditions of the lower atmosphere ~~-~~favor the accumulation of nuclides~~ is favored by near-stable conditions of the lower atmosphere~~. From this perspective, we can infer that $^{214}Pb_{eq}$~~S_β~~ and $^{212}Pb_{eq}$~~L_β~~ we~~a~~re coexistent when local emission and atmospheric stability are dominant compared with~~to~~ long-range transport. This last process can be identified when the long-lived~~L_β~~ is negligible (^{212}Pb and ^{212}Bi is completely decayed after 50 hours) and air masses could be "*recent*" or "*aged*" in presence or not, respectively, of the short-lived progeny~~S_β~~. This study cannot, at the moment~~of course~~, ~~deeply~~ analyz~~s~~e these issues since the LLDs of the two minor components (long-lived and near-constant progenies) are still too high and a longer dataset is mandatory for providing a solid statistics. ~~S_β.~~

Nevertheless, back-trajectories and the observed absolute humidity provided ~~A~~additional information~~ can be obtained considering back-trajectories and the observed absolute humidity~~~~This interpretation can be supported describing two case-study situations (Fig. 4)~~. The occurrence of periods characterized by high $^{214}Pb_{eq}$ - $^{212}Pb_{eq}$ ratios (above 4 and 8 during the different seasons) or by significant C_β activities (Fig. 4a) were, in fact, associated with atmospheric stability and advection of flows arriving from the open sea or from the glaciers. The first driving factor is the persistence or not of winds below 4 m s^{-1} and this distinction wa~~i~~s controlled by atmospheric stability. It is important to remember, in this case, that while low wind speeds reduce the efficiency of local radon emanation, high wind speed contrasts accumulation of nuclides in the air but favors radon exhalation (see Sect. 2.2~~XX~~). Atmospheric stability can be traced looking at the residence time of air masses (estimated for 500 and 1000 m altitude backtrajectories) above Svalbard islands (we considered an area of 350 km radius) in the last 5 days (Fig. 4c~~b~~). This information is not completely exhaustive since it ~~doesn't~~does not consider the vertical intrusion of air masses through the inversion layer. The decoupling between the above-inversion and below-inversion air circulation in the fiord seemed to play an important role especially during the summer period when a long wind-calm window (about 20 days in August) ~~can be detected~~occurred. During this event~~window~~ the radon-progeny ratio was permanently high but the residence time of air masses was very low (less than 12 hours with occasional spikes).

The dynamics of the inversion layer in the fiord system

will be investigated in the next future considering additional observations that can describe the fiord system better than a coarse-resolution model like HYSPLIT. The evolution of absolute humidity provided s~~S~~ome confirmations about the importance of this process ~~can be obtained from the evolution of absolute humidity ~~(Fig.4b~~c~~). The general increasing trend over the whole campaign was, in fact, ~~-~~combined to accumulation windows, probably related to atmospheric stability, and to abrupt decrements (more than 1~~0.~~ g m-3) that were probably associated with glacier flows. These slope flows, with a katabati~~y~~c behavior indicated also ~~, were ~~by~~coupled to~~ high wind speed (more than 8 m s-1)~~, and they~~were coincident with significant C_β activities.

~~This interpretation can be supported describing two case-study situations (Fig. 4). The first example shows the contribute of processes related to long-range transport. We observed two advective phases (when wind speed was higher than 1 m s^{-1} before 1 May) followed by a relatively-stable situation. The L_{β} increased (about 20%), especially during the third phase, evidencing that, although the emanation conditions of the ground were unfavorable during all the period, the radon emanation was not negligible. All of the air masses were persistent over the Arctic Ocean for at least 5 days and the contact with terrestrial surfaces is significant only in the third phase. While the overpass on Svalbard was limited to 10-20 hours in the first two situations, the third phase, dominated by atmospheric stability (wind-calm), was characterized by a persistence over the islands of about 48 hours including a heavy compression episode occurring close to coast 24 hours before the contact in Ny Ålesund. The difference between the first two phases could be represented by the stratification of the atmosphere close to the study site. While the first phase was characterized by a homogeneous flying altitude of the air mass, the second situation was influenced by the rise of sea-lying air masses potentially depleted of haze-related isotopes. While mixtures of the first phase lay in between SC and CS classes, the second and the third ones can be classified as HiL with a decreasing short-to-long progenies ratio. This feature controlled the presence of L_{β} close to the measuring station and the absence of C_{β} at lower altitudes above the continental areas. The occurrence of near-stable conditions in the atmosphere controls, moreover, the accumulation of nuclides. This behavior was slightly visible when emanation is very low, but it was clearly identified in the second episode occurring between June 6 and 11 (Fig. 4). The accumulation of S_{β} and L_{β} was, in this case, consistent with near-stable conditions of the lower atmosphere and potential emitting areas are 50 hours far from the measuring station. The peak situation can be classified as SL indicating that the short-to-long ratio is proportional to the contribute of long-range transport, of "*recent*" air masses (originated up to 20 days before), instead of local emission. This statement is supported by this example thus the considered air mass was over continental areas at lower latitudes and altitudes 3-4 days before the contact with Ny Ålesund. The presence of C_{β} cannot be investigated at this stage of the study due to the very long residence time of those nuclides in the atmosphere.~~ The availability of a longer dataset coupled to a reliable calibration of this technique are~~is~~ the first steps~~step~~ that must be addressed in order to obtain more a detailed description of complex processes in polar areas~~approach this issue~~.

4 Conclusions

The detection of β emission from airborne particles with a high-time resolution offers the opportunity to increase the capability of studying atmospheric processes in polar areas. The reduction of soil exhalation during spring may appear as a limitation, but it represents an important challenge. The composition of the radon progeny in the Arctic region (above 70°N), defined for the first time with a high-time resolution, supported the identification of air masses dominated by long-range transport (with life up to 20 days and more than 20 days) in presence or not of near-constant radionuclides instead of long and short lived progenies. This study supports to extend this approach from the definition of the accumulation processes involving isotopes present in the lower atmosphere, to the identification of the stability conditions of the lower atmosphere, to gather information about air masses and the soil-exhalation conditions. Two different emanation periods were defined in accordance to the permafrost occurrence at the ground. Furthermore, accumulation windows were recognized coherently to the meteo-climatic conditions occurring at the study site. This preliminary attempt must be continued with a longer time series in order to statistically analyze the correlation between radioactivity and mixing state of the lower atmosphere. However, we are confident that coupling this method with traditional chemical determinations on gases and aerosols, a more complete picture of pollutant dynamics in the Arctic region can be achieved.

5 Acknowledgments and Data

This study was supported by the logistic service provided by the Earth System Science and Environmental Technologies Department of the National Research Council of Italy. We would like to thank EUMETSAT for providing data products concerning the soil moisture content and AWI for the available dataset about the permafrost thermal profile. The authors gratefully acknowledge the NOAA Air Resources Laboratory (ARL), for the provision of the HYSPLIT transport and dispersion model used in this publication, and NCEP, for providing the Global Data Assimilation System (GDAS). This manuscript was language-proofed by Lena Rettori.

References

AMAP: AMAP Assessment 2009: Radioactivity in the Arctic. Arctic Monitoring and Assessment Programme (AMAP), Oslo, Norway, ISBN 13 978-82-7971-059-2, 2010.

Baskaran M.: Radon: A Tracer for Atmospheric Studies, in Radon: A Tracer for Geological, Geophysical and Geochemical Studies, Springer, Switzerland, 63-81, doi:10.1007/978-3-319-21329-3, 2016.

Baskaran M., and Shaw G. E.: Residence time of arctic haze aerosols using the concentrations and activity ratios of Po, Pb and Be, Aerosol Sci., 32, 443-452, 2001.

Bocanegra R., and Hopke P. K.: Radon adsorption on activated carbon and the effect of some airborne contaminants, Sci. Total Environ., 76, 193-202, doi:0048-9697/88/$03.50, 1988.

Brocca L., Crow W. T., Ciabatta L., Massari C., de Rosnay P., Enenkel M., Hahn S., Amarnath G., Camici S., Tarpanelli A., and Wagner W.: A review of the Applications of ASCA Soil Moisture Products, IEEE J. Sel. Topics Appl. Earth Observ., 10 (5), 2285-2306. 2017

Chambers S. D., Hong S. B., Williams A. G., Crawford J., Griffiths A. D., and Park S. J.: Characterising terrestrial influences on Antarctic air masses using Radon-222 measurements at King George Island, Atmos. Chem. Phys., 14, 9903–9916, 2014.

Chambers S. D., Williams A. G., Conen F., Griffiths A. D., Reimann S., Steinbacher M., Krummel P. B., Steele L. P., van der Schoot M. V., Galbally I. E., Molloy S. B., and Barnes J. E.: Towards a universal “baseline” characterisation of air masses for high- and low-altitude observing stations using Radon-222, Aerosol Air Qual. Res., 16, 885–899, 2016.

Chambers S. D., Williams A. G., Crawford J., and Griffiths A. D.: On the use of radon for quantifying the effects of atmospheric stability on urban emissions, Atmos. Chem. Phys., 15, 1175–1190, 2015.

Chambers S. D., Williams A. G., Zahorowski W., Griffiths A. D., and Crawford J.: Separating remote fetch and local mixing influences on vertical radon measurements in the lower atmosphere, Tellus~~,~~ ~~Ser.~~ B, 63, 843–859, 2011.

~~Chambers 2016Chambers, SD, Williams, AG, Conen, F, Griffiths, AD, Reimann, S, Steinbacher, M,~~

~~Krummel, PB, Steele, LP, van der Schoot, MV, Galbally, IE, Molloy, SB, and Barnes, JE. 'Towards a universal "baseline" characterisation of air masses for high- and low-~~

~~altitude observing stations using Radon-222'. Aerosol and Air Quality Research 16,885–899, 2016.~~

Chun J.: On the research needed to better characterise natural radioactivity accumulated in the Arctic by long-range atmospheric transport, Radiat. Prot. Dosim., 158(4), 369 –372, 2014.

Cowpertwait P. S. P., and Metacalfe A. V.: Introductory Time Series with R (2nd Ed), Springer, Baltimore, USA, doi:10.1007/978-0-387-88698-5, 2009.

Esau I., and Repina I.: Wind Climate in Kongsfjorden, Svalbard, and Attribution of Leading Wind Driving Mechanisms through Turbulence-Resolving Simulations, Adv. Meteorol., 568454, pp 16, doi:10.1155/2012/568454, 2012.

Di Liberto L., Angelini F., Pietroni I., Cairo F., Di Donfrancesco G., Viola A., Argentini S., Fierli F., Gobbi G., Maturilli M., Neuber R., and Snels M.: Estimate of the Arctic Convective Boundary Layer Height from Lidar Observations: A Case Study, Adv. Meteorol., 2012, 851927, doi:10.1155/2012/851927, 2012.

Duenas C., Perez M., Fernandez M. C., and Carretero J.: Radon concentrations in surface air and vertical atmospheric stability of the lower atmosphere, J. Environ. Radioact., 31, 87–102, 1996.

EUMETSAT: ASCAT Product Guide, EUM/OPS-EPS/MAN/04/0028, 2015.

Griffith A. D., Parkes S. D., Chambers S. D., McCabe M. F., and Williams A. G.: Improved mixing height monitoring through a combination of lidar and radon measurements, Atmos. Meas. Tech., 6, 207–218, 2013.

Griffiths A. D., Chambers S. D., Williams A.G., and Werczynski S.R.: Increasing the accuracy and temporal resolution of two-filter radon–222 measurements by correcting for the instrument response, Atmos. Meas. Tech., 9, 2689-2707, 2016.

Islam G. S., and Haque A. K. F.: Measurement of mixed radon and thoron daughter concentrations using alpha and beta activities filtered from air, Radiat. Meas., 23(4), 737–742, 1994.

Lee C. J., and Burgess P. H.: The examination, testing and calibration of portable radiation protection instruments, Measurement Good Practice Guide, 14, NPL, Teddington, UK, 2014.

~~Levin 2002~~

Levin~~,~~ I., Born~~,~~ M., Cuntz~~,~~ M., Langendörfer~~,~~ U., Mantsch~~,~~ S., Naegler~~,~~ T., Schmidt~~,~~ M., Varlagin~~,~~ A., Verclas~~,~~ S., and ~~and~~ Wagenbach~~,~~ D.: ~~"~~Observations of atmospheric variability and soil exhalation rate of Radon-222 at a Russian forest site: Technical approach and deployment for boundary layer studies~~"~~~~,~~. Tellus B, 54~~B~~, 462-475, 2002.

Mazzola M., Tampieri F., Viola A. P., Lanconelli C., and Choi T.: Stable boundary layer vertical scales in the Arctic: observations and analyses at Ny-Alesund, Svalbard, Q. J. R. Meteorol. Soc., 142, 1250–1258, doi:10.1002/qj.2727, 2016.

Paatero J., Buyukay M., Holmén K., Hatakka J., and Viisanen Y.: Seasonal variation and source areas of airborne lead-210 at Ny-Ålesund in the High Arctic, Polar Res., 29, 345–352, 2010.

Paatero J., Hatakka J., Mattsson R., and Lehtinen I.:~~et al 200~~ A comprehensive station for monitoring atmospheric radioactivity, Radiati~~i~~. Prot. ~~ection~~ D~~d~~osim.~~etry~~, 54~~,~~ (1), 33-39, 1994.

~~Paatero J., Buyukay M., Holmén K., Hatakka J., and Viisanen Y.: Seasonal variation and source areas of airborne lead-210 at Ny-Ålesund in the High Arctic, Polar Res., 29, 345–352, 2010.~~

Pasini A., and Ameli F.: Radon short range forecasting through time series preprocessing and neural network modeling, Geophys. Res. Lett., 30(7), 1386, 2003.

Pasini A., Salzano R., and Attanasio A.: Modeling radon behavior for characterizing and forecasting geophysical variables at the atmosphere-soil interface, in Recent trends in modelling of environmental contaminants, edited by D. Sengupta, Springer, New Delhi, 213–237, 2014.

Paulik C., Melzer T., Hahn S., Bartsch A., Heim B., Elger K., and Wagner W.: Circumpolar surface soil moisture and freeze/thaw surface status remote sensing products (version 4) with links to geotiff images and NetCDF files (2007-01 to 2013-12). Department of Geodesy and Geoinformatics, TU Vienna, doi:10.1594/PANGAEA.832153, 2014.

Perrino C., Febo A., and Allegrini I.: A new beta gauge monitor for the measurement of PM10 air concentration, in EMEP-WMO workshop on fine particles—emissions, modelling and measurements, edited by J. E. Hanssen, EMEP/CCC-Report 9/2000, NILU, Kjeller, 147–152, 2000.

Perrino C., Pietrodangelo A., and Febo A.: An atmospheric stability index based on radon progeny measurements for the evaluation of primary urban pollution, Atmos. Environ., 35(31), 5235–5244, 2001.

Porstendorfer J.: Properties and behaviour of radon and thoron and their decay products in the air, J. Aerosol Sci., 25(2), 219–263, 1994.

Salzano R., Pasini A., Casasanta G., Cacciani M., and Perrino C.: Quantitative Interpretation of Air Radon Progeny Fluctuations in Terms of Stability Conditions in the Atmospheric Boundary Layer, Bound-Lay. Meteorol., 160(3), 529–550, doi:10.1007/s10546-016-0149-6, 2016.

Samuelson C., Hallstadius L., Persson B., Hedvall R., Holm E., and Forkman B.: 222Rn d 210Pb in the Arctic summer air, J. Environ. Radioact., 3, 35-54, 1986.

Sesana L., Caprioli E., and Marcazzan G. M.: Long period study of outdoor radon concentration in Milan and correlation between its temporal variations and dispersion properties of atmosphere, J. Environ. Radioact., 65, 147–160, 2003.

Stein A. F., Draxler R. R., Rolph G. D., Stunder B. J. B., Cohen M. D., and Ngan F.: NOAA's HYSPLIT atmospheric transport and dispersion modeling system, Bull. Amer. Meteor. Soc., 96, 2059-2077, doi:10.1175/BAMS-D-14-00110.1, 2015.

St~~h~~ohl~~Sthol~~ A.: Characteristics of atmospheric transport into the Arctic troposphere, J. Geophys. Res., 111, D11306, doi:10.1029/2005JD006888, 2006.

Suzuki T., Nakayama N., Igarashi M., Kamiyama K., and Watanabe O.: Concentrations of 210Pb and 218Po in the atmosphere of Ny-Alesund, Svalbard, Mem. Natl Inst. Polar Res., Spec. Issue, 51, 233-237, 1996.

Veleva B., Valkov N., Batchvarova E., and Kolarova M.: Variation of short-lived beta radionuclide (radon progeny) concentrations and the mixing processes in the atmospheric boundary layer, J. Environ. Radioact., 101, 538–543, 2010.

~~Wada~~ Wada~~,~~ A., Muramaya~~,~~ S., Kondo~~,~~ H., Matsueda~~,~~ H., Sawa~~,~~ Y., and Tsuboi~~,~~ K.:~~, 2010.~~ Development of a compact and sensitive electrostatic radon-222 measuring system for use in atmospheric observation,~~.~~ J. Meteorol. Soc. Jpn., 88 (2), 123-~~e~~134. http://dx.doi.org/10.2151/jmsj.2010-202, 2010.

~~Willams and Chambers 2016 Williams, AG, and Chambers, SD. 'A history of radon measurements at Cape Grim', Baseline Atmospheric Program (Australia) History and Recollections (40th Anniversary Special Edition), 131-146, 2016.~~

Zhang W., Chen J., Ungar K., and Cooke M.: Estimation of the Arctic aerosols from local and long-range transport using relationships between 210Pb and 212Pb atmospheric activity concentrations, J. Environ. Radioact., 141, 123-129, doi:10.1016/j.jenvrad.2014.12.008, 2015.

Zhuo W., Guo Q., Chen B., and Cheng G.: Estimating the amount and distribution of radon flux density from the soil surface in China, J. Environ. Radioact., 99, 1143–1148, 2008.

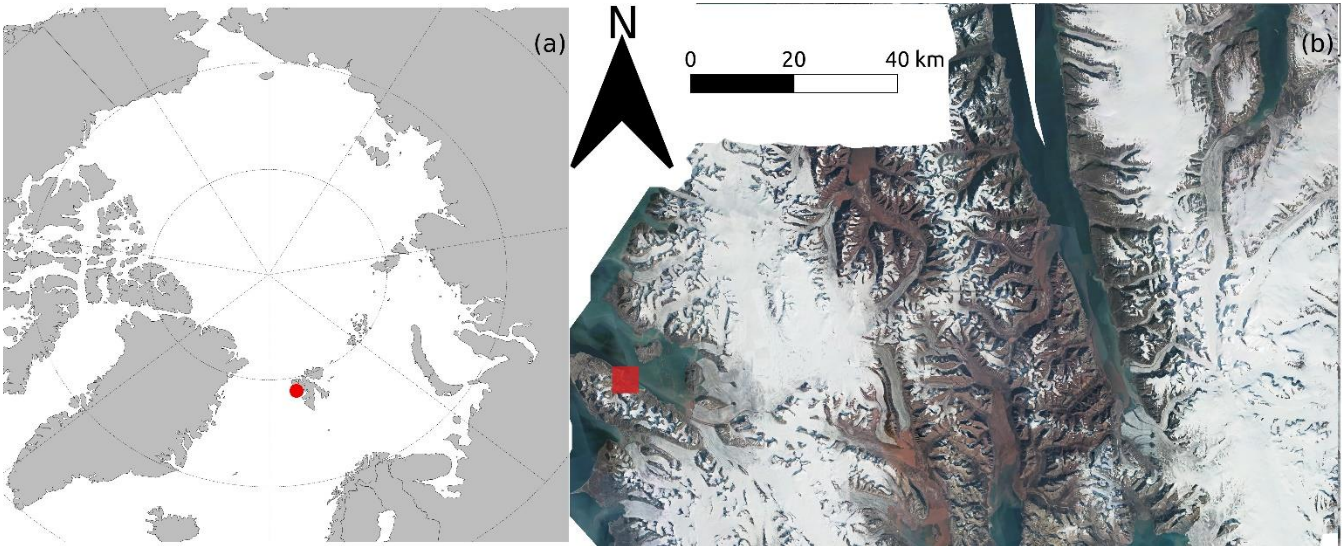

Figure 1: Location map (a) of Ny Ålesund (Svalbard Islands, Norway) and zoom (b) on the Gruvebadet observatory (~~Courtesy~~ courtesy of Norwegian Polar Institute).

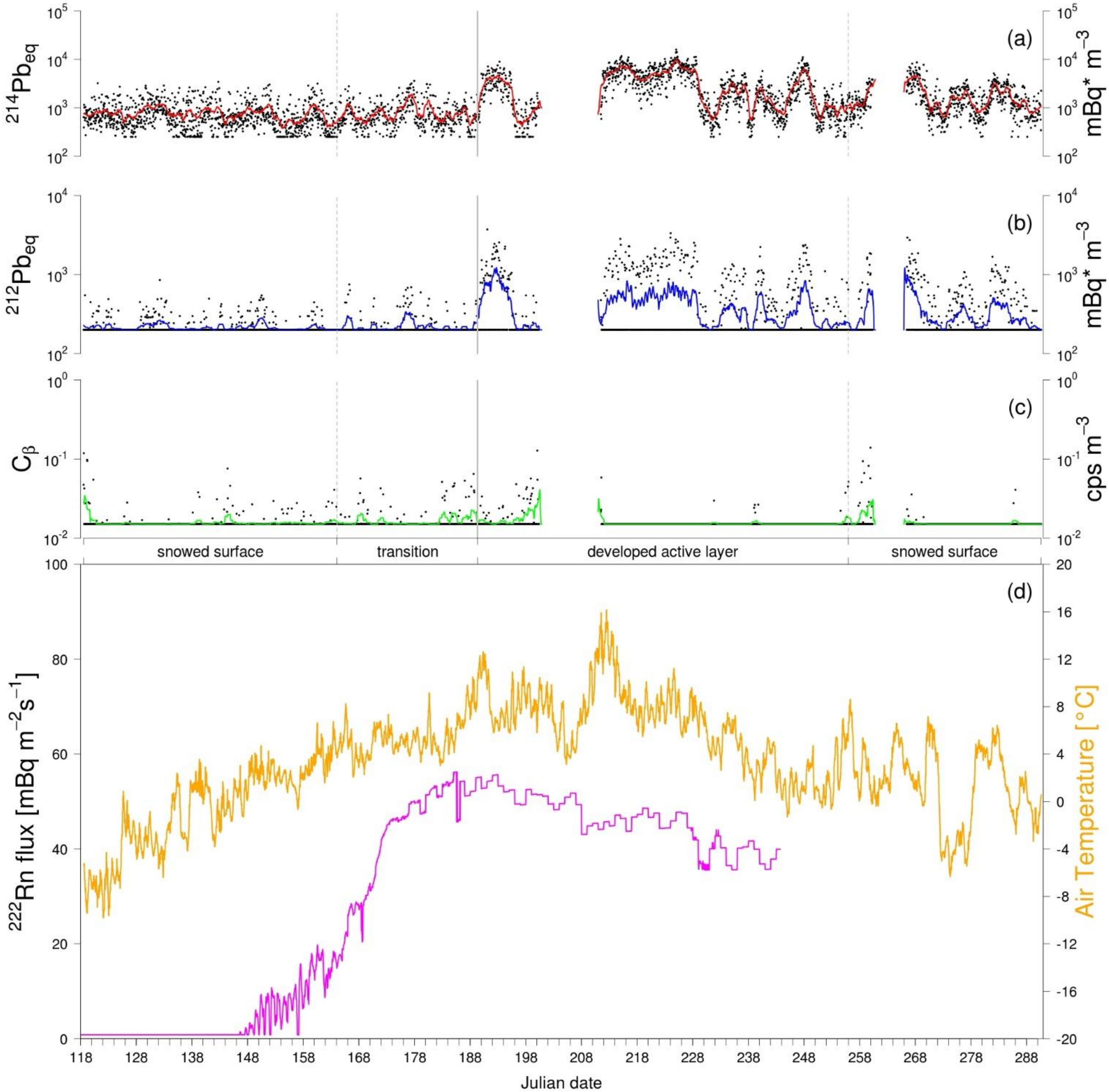

Figure 2: Variability of the three estimated radioactive components (black points) during the campaign at Ny Ålesund in 2015. Coloured lines show the smoothed trend of $^{214}Pb_{eq}$ (a), $^{212}Pb_{eq}$ (b) and C_β (c). Activities are represented assuming equilibrium between progenies and a bold calibration estimation (*). Comparison (d) with the simulated s~~S~~oil flux (~~black line~~magenta) ~~versus airborne natural radioactivity (colored lines) in Ny Ålesund. The~~and the air temperature (orange~~grey~~) ~~was measured at the CCT Tower facility~~. Note the log scale for panels a, b and c.

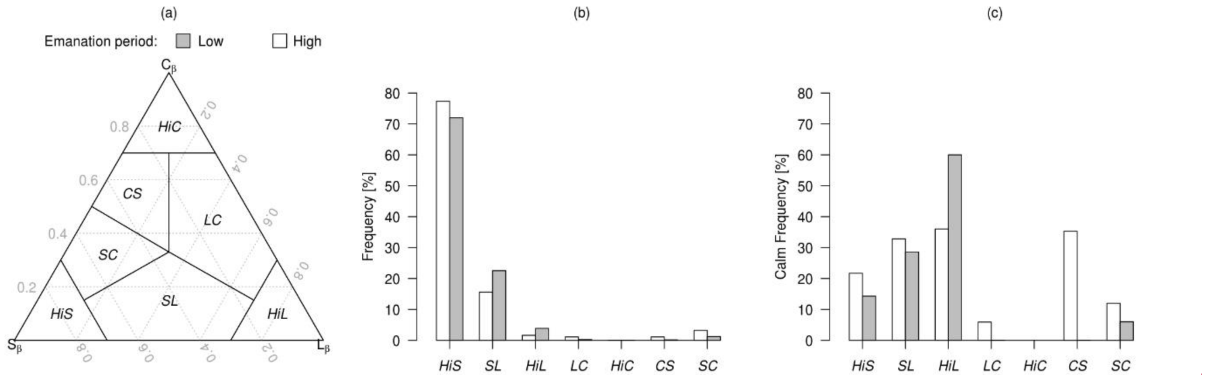

(a)
Emanation period: Low High
C_β
S_β
L_β
HiC
CS
LC
SC
SL
HiS
HiL
0.2
0.4
0.6
0.8
(b)
Frequency [%]
HiS SL HiL LC HiC CS SC
(c)
Calm Frequency [%]
HiS SL HiL LC HiC CS SC

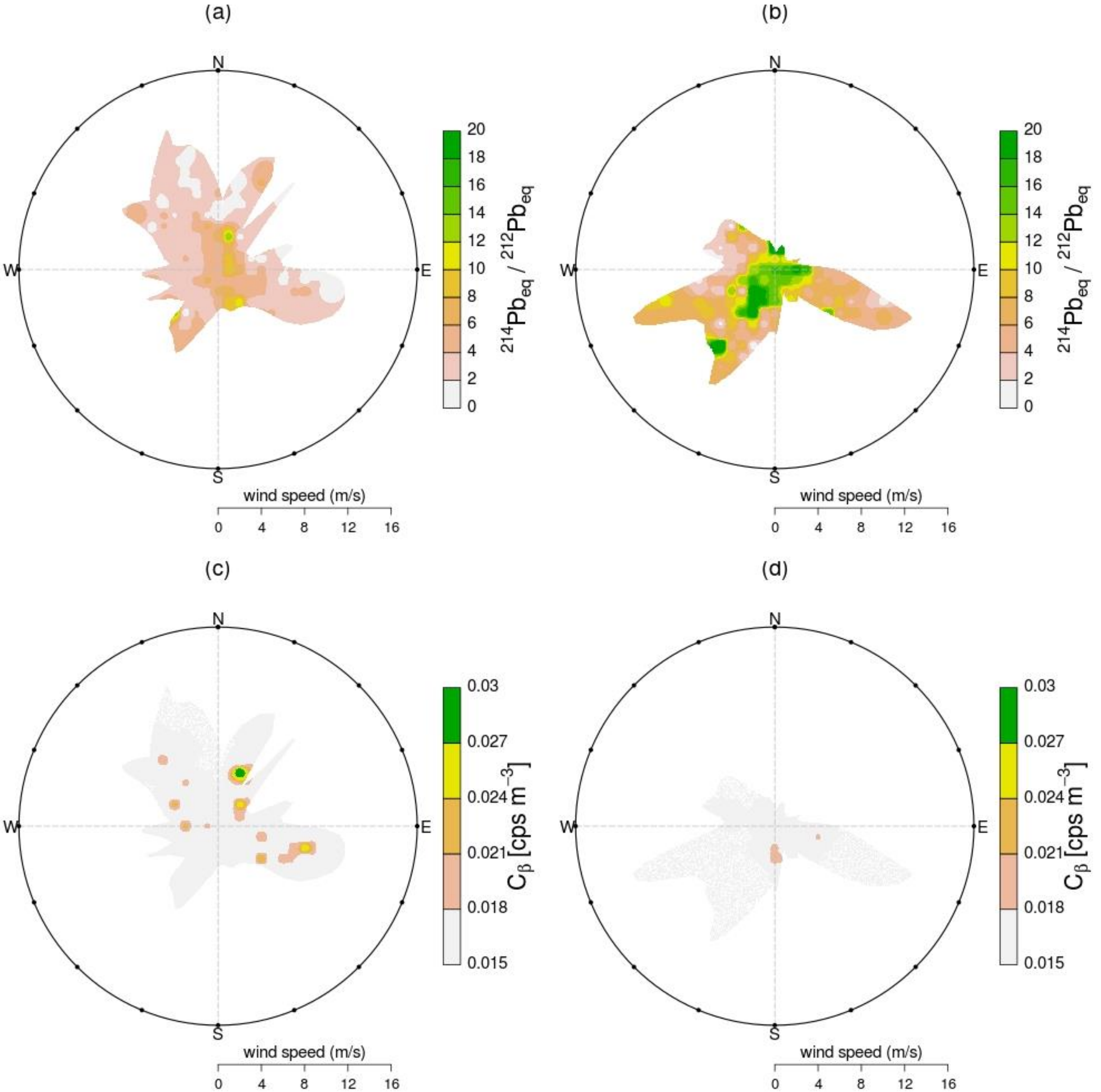

Figure 3: Polar bivariate plots of $^{214}Pb_{eq}$ - $^{212}Pb_{eq}$ (a, b) and C_β (c, d) during the two different emanation periods. The low emanation period (a, c) and the high emanation period (b, d) are based on hourly observations assuming equilibrium between radon progenies.~~Classification of radon-progeny mixtures (a), occurrence of the different isotopic compositions (b) and association between the different mixtures under wind-calm conditions (c). Classes were defined considering the relative amount of each component.~~

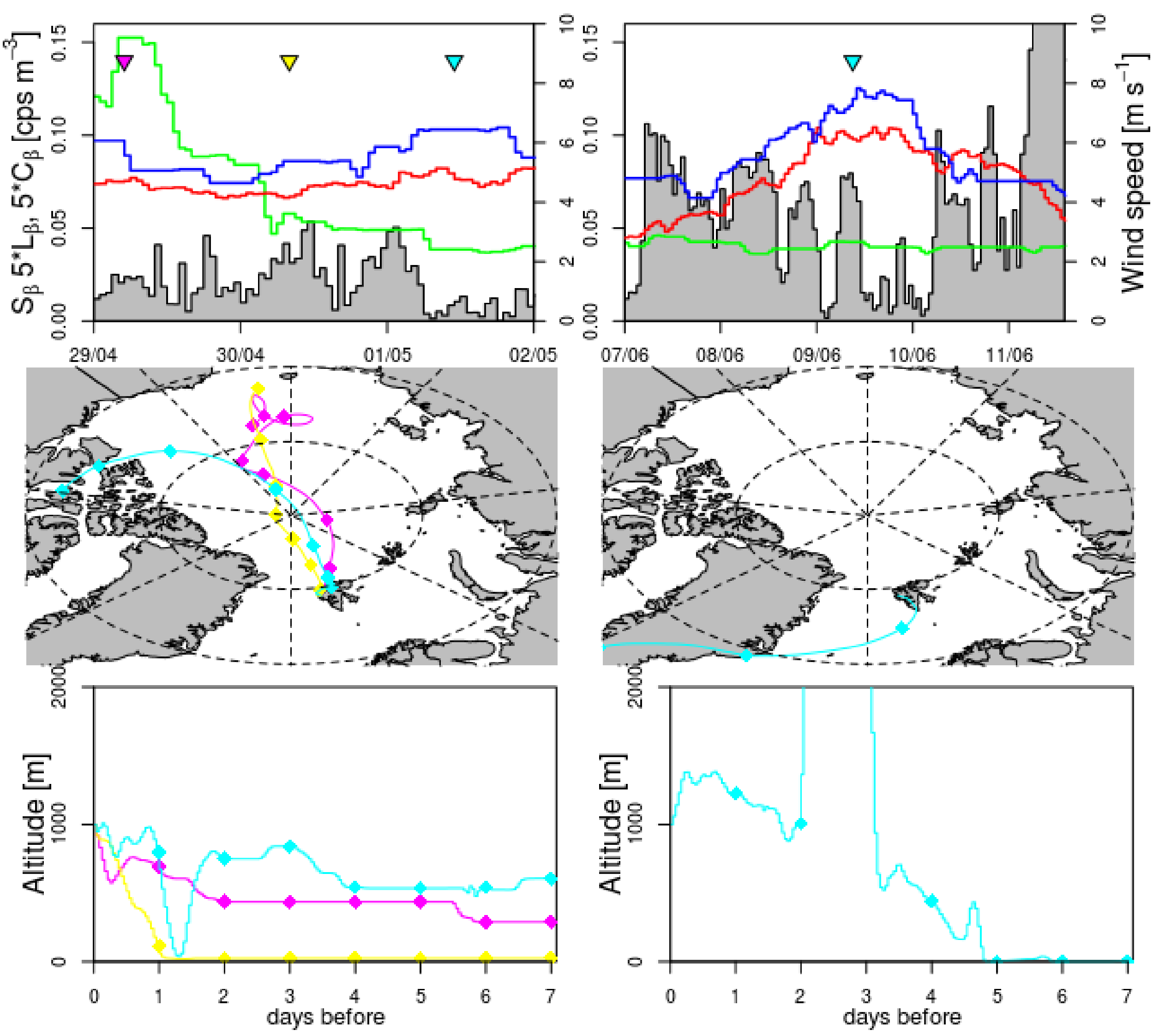

S_β 5*L_β, 5*C_β [cps m^-3]
Wind speed [m s^-1]
29/04
30/04
01/05
02/05
07/06
08/06
09/06
10/06
11/06
Altitude [m]
days before

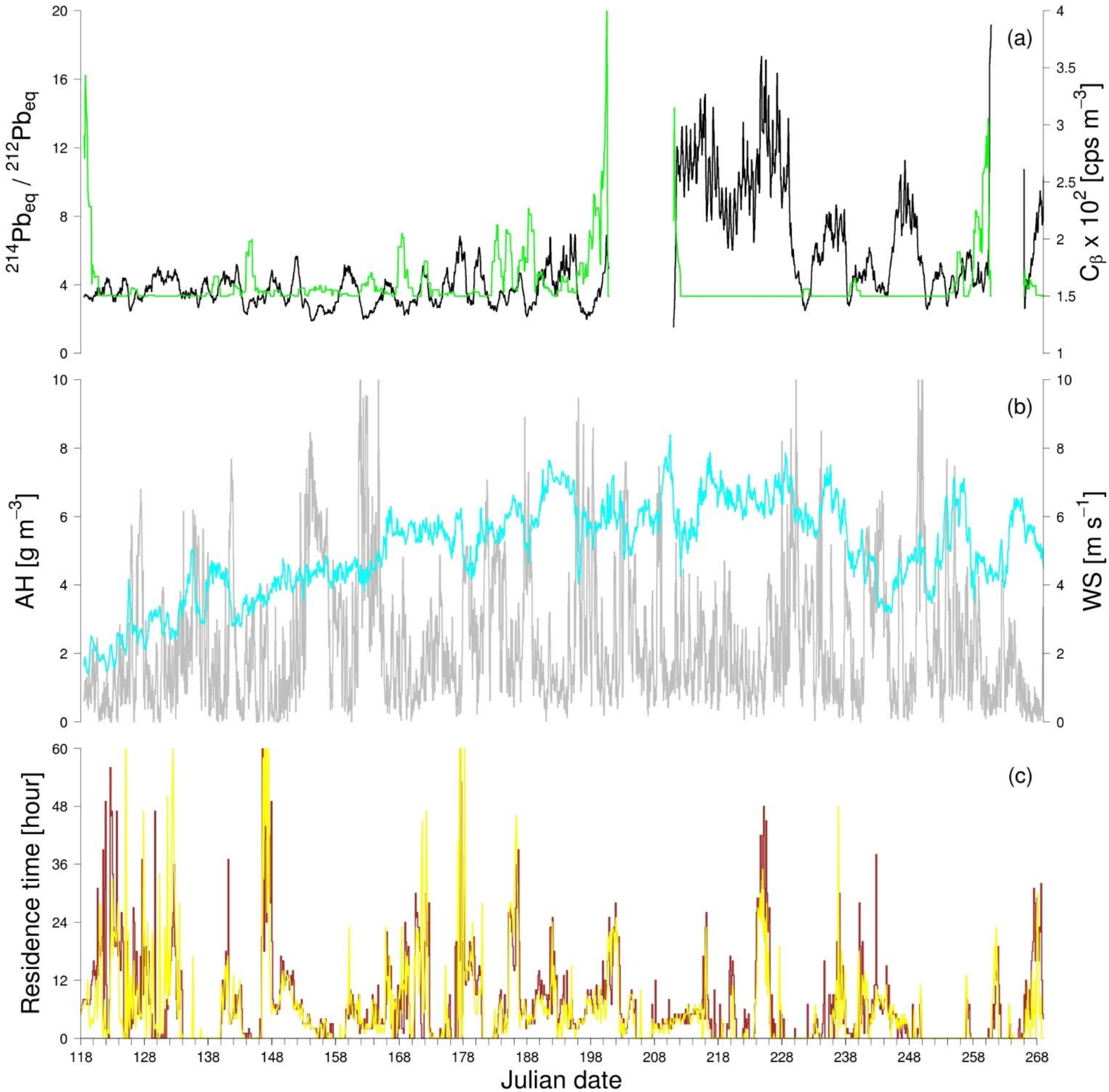

Figure 4: Evolution of the isotopic composition of radon progeny (a) compared ~~to~~ with meteorological parameters (b) and the residence time of air masses close to Svalbard islands (c). The $^{214}Pb_{eq}$ - $^{212}Pb_{eq}$ ratio (black) is reported with the relative counts of C_β (green). The w~~w~~ind speed~~conditions~~ (grey~~top~~) and the absolute humidity (cyan) are associated with the residence time of air masses over Svalbard (within a distance of 350 km) at different altitudes: 500 m a.s.l. (red) and 1000 m a.s.l. (yellow).~~, specific back-~~

~~**trajectories in terms of path (middle) and altitude (bottom). One example is referred to long-range transport at the beginning of the melting season (left) and one to local emission (right).**~~